Corrosion Science 92 (2015) 301–308

Contents lists available at ScienceDirect

Corrosion Science

journal homepage: www.elsevier.com/locate/corsci

Correlation between sensitisation and pitting corrosion of AISI 403 martensitic stainless steel

I. Taji, M.H. Moayed *, M. Mirjalili

Metallurgical and Materials Engineering Department, Faculty of Engineering, Ferdowsi University of Mashhad, Mashhad 91775-1111, Iran

ARTICLE INFO

Article history:
Received 21 September 2014
Accepted 9 December 2014
Available online 2 January 2015

Keywords:
A. Stainless steel
B. Polarisation
C. Pitting corrosion
C. Intergranular corrosion

ABSTRACT

In this work, the effect of different tempering temperatures on the degree of sensitisation (DOS) and pitting corrosion of AISI 403 martensitic stainless steel is studied. The specimens were annealed at 1050 °C and then tempered at 300, 450, 550, 650 and 750 °C. The influence of sensitisation on pitting behaviour is investigated by electrochemical and microstructural studies. The DOS was measured using modified solution for martensitic stainless steel in double loop electrochemical potentiodynamic (DL-EPR) technique. Electrochemical studies revealed that the highest DOS and the lowest pitting potential are coincided in the specimen tempered at 550 °C.

1. Introduction

Martensitic stainless steels containing more than 11% chromium are extensively used in chemical and power industries, steam generators, pressure vessels, cutting tools, mining equipment and compressor blades [1–4]. This type of stainless steel is generally heat treated to provide a good combination of mechanical properties and moderate corrosion resistance. This process is often involved solution annealing treatment to obtain an austenitic structure followed by cooling to have a martensitic transformation [2–4]. Annealed martensitic parts need subsequent tempering according to their application requirements.

Inappropriate selection of the tempering conditions can lead to precipitation of chromium-rich carbides in the vicinity of grain boundaries [5–10] and martensitic laths [7–10]. Thus, the chromium depleted zones are formed adjacent to the carbides and consequently sensitisation is happened. However, when the tempering time is prolonged or the temperature increases, the sensitization effect vanishes as a result of chromium diffusion from the interior parts of the grains to heal the depleted zones [3,7].

There are several methods to measure the degree of sensitisation or intergranular corrosion. In the recent decades, the electrochemical techniques especially double loop electrochemical potentiodynamic reactivation (DL-EPR) is developed to provide a rapid, quantitative and non-destructive method [5,6,11]. DL-EPR technique was initially developed for austenitic stainless steels [6,11–13] and then improved for ferritic [5,14], duplex [15,16] and martensitic stainless steels [7,9]. In the DL-EPR technique, specimen is first polarised anodically from the corrosion potential to the passive region in order to form a continuous passive layer on the whole surface. Then the scan direction is reversed to reactivation occur. During the reactivation of a non-sensitised steel, the passive film remains intact or only a negligible small increase in the reactivation current density (I_r) might be observed, while reactivation current density of sensitised samples is increased due to the weaker passive film formed on the chromium depleted zones [6,17]. Fig. 1 shows the schematic diagram of double loops in the DL-EPR test. In this technique, The ratio of the maximum current or the whole charge generated in the reactivation loop (I_r or Q_r) to the maximum current or the whole charge generated in the activation loop (I_a or Q_a) is introduced as the degree of sensitisation (DOS) [6,17,18].

Pitting corrosion is an important localised corrosion occurred in the steels showed active–passive behaviour. Due to passive layer susceptibility to local breakdown in aggressive ions presence, pitting corrosion occurred and consequently underlying metal dissolution would be accelerated [19,20]. Pit nucleation mostly occurs at the surface active sites such as inclusions [21–23], or any place with a diminished passive film, such as chromium depleted zones in the sensitised stainless steels [14,24]. A tempering map illustrating the conditions led to sensitisation happen in 403 martensitic stainless steels is proposed by Lim et al. [3]. With modifying Strauss technique, they suggested that the highest DOS of 403 martensitic stainless steel occurred in alloy tempered at 660 °C. However, Alonso-Falleiros et al. [7] investigated the intergranular corrosion of 410 martensitic stainless steel by electrochemical tests and found that the highest DOS occurs in the specimen tempered at 550 °C.

* Corresponding author. Tel./fax: +98 511 8763305.
E-mail address: mhmoayd@um.ac.ir (M.H. Moayed).

http://dx.doi.org/10.1016/j.corsci.2014.12.009
0010-938X/

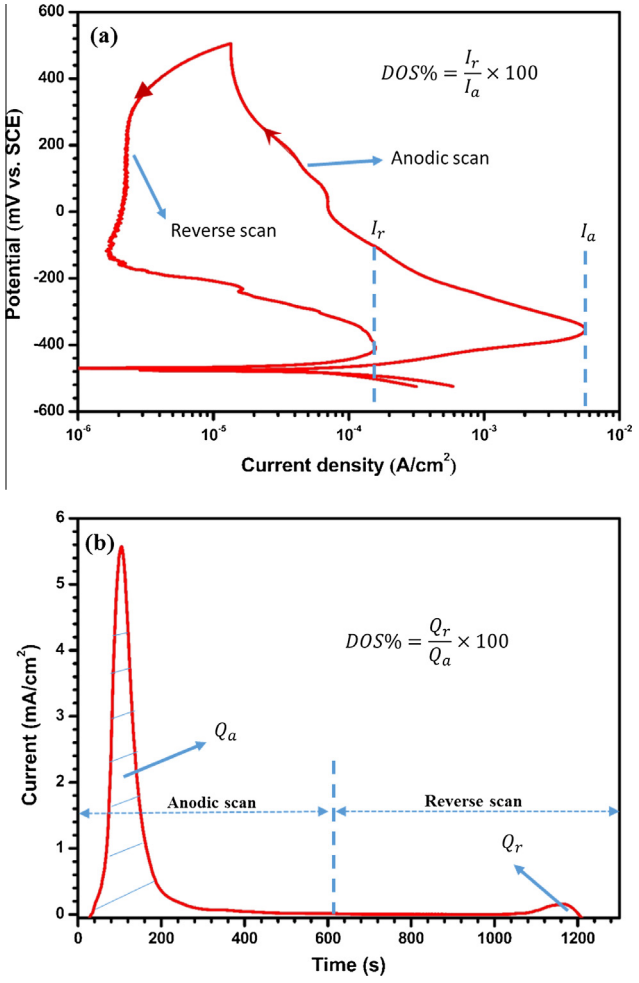

Fig. 1. Schematic diagrams of the DL-EPR experiment: (a) potential vs. time diagram which indicates the amounts of I_a and I_r, (b) current vs. time diagram which indicates the amounts of Q_a and Q_r that equal to the areas under the activation and reactivation peaks, respectively. The ratio of I_r/I_a or Q_r/Q_a indicates the degree of sensitisation (DOS).

The influence of sensitisation on pitting corrosion resistance of 430 ferritic stainless steel has been studied by Paroni and co-workers [14]. They claimed that the resistance to pitting corrosion is reduced due to sensitisation occurred in the alloy. It is in agreement with Aquino et al. [25] who suggested that in super-martensitic stainless steel weldment, regions suffered from higher degree of sensitisation reveal lower pitting potential rather than non-sensitised zones.

In the present work, the effect of various tempering temperatures on the sensitisation and pitting corrosion of AISI 403 martensitic stainless steel is studied. DL-EPR, potentiodynamic, potentiostatic and microstructural techniques are used in order to find a correlation between the sensitisation and pitting behaviour of this steel in 3.5 wt.% NaCl solution. Moreover, the electrolyte solution of the DL-EPR technique is modified for this type of stainless steel. However, it is not the intention of this work to introduce a new test procedure for DL-EPR method.

2. Experimental procedures

2.1. Samples preparation

The chemical composition of AISI 403 martensitic stainless steel used in this study is given in Table 1. The steel was cut in the form of cubic specimens with dimensions of 1 cm. All specimens then were solution annealed at 1050 °C for 1 h followed by air cooling. Next, samples were tempered at 300 °C, 450 °C, 550 °C, 650 °C and 750 °C for 1 h and cooled in air. Afterwards, samples were passivated at 0.1 M Na_2SO_4 solution at the anodic potential of 850 mV vs. SCE for 900 s to grow the passive film. Performing this procedure prior to the specimens be mounted is proved to prevent crevice corrosion. Working electrodes, with 1 cm^2 exposed area, were prepared by mounting the samples with a self-cure epoxy resin. The electrical contacts were connected through a threaded hole at the back of the specimen. For each electrochemical experiment, the specimen surface was ground by silicon carbide (SiC) emery papers from 60 to 1200 mesh, then rinsed with ethanol, and finally dried with warm air.

2.2. Surface morphology

Microstructural characterisation was performed utilising optical microscopy (OM) and scanning electron microscope (SEM) model LEO VP 1450. For this purpose, the exposing surface of the specimens were ground by silicon carbide (SiC) emery papers from 60 to 1200 grit and then were polished by 0.05 μm alumina slurry to make mirror surface. Afterwards, the samples were electrochemically etched at 10 wt.% aqueous solution of oxalic acid under a current density of 1 A cm^{-2} for 90 s according to the ASTM A-262 practice A. In addition, the presence of MnS inclusions were analysed by energy dispersive X-ray spectroscopy (EDS).

2.3. Electrochemical techniques

All electrochemical techniques were conducted by means of Gill AC automated potentiostat (ACM instruments). The electrochemical cell was a 250 mL beaker open to air filled with 100 mL of the test solution. Saturated calomel electrode (SCE) was used as a reference electrode for all experiments. The auxiliary electrode was a bright platinum sheet with 2 cm^2 area. All the experiments were conducted at 20 ± 2 °C.

The DL-EPR tests were performed to determine the DOS of the 403 martensitic stainless steel exposed to different tempering conditions. In these experiments, five different solutions were used for evaluating the DOS of 403 martensitic stainless steel in DL-EPR test (as listed in Table 2).

In DL-EPR experiments, the potential was swept from 50 mV lower than open circuit potential (OCP) up to 550 mV vs. SCE and then reversed to the initial potential with the scanning rate of 100 mV min^{-1}. The DOS values were calculated using the ratio of the entire charge of reactivation curve (Q_r) to the entire charge of activation one (Q_a), as below [18]:

$$\mathrm{DOS}\ (\%) = \frac{Q_r}{Q_a} \times 100 \qquad (1)$$

Before DL-EPR polarisation, the specimens were immersed into the solution for 600 s to reach the steady state condition. DL-EPR tests for each sample were repeated four times to ensure the reproducibility.

Pitting corrosion of the samples was investigated by means of potentiodynamic and potentiostatic polarisation techniques in 3.5 wt.% sodium chloride (NaCl) solution. The solution was prepared using an analytical reagent of sodium chloride and distilled water. In the potentiodynamic method, samples were polarised from 50 mV below the OCP to the potentials indicating the pitting corrosion. The scanning rate was 30 mV min^{-1}. The pitting potential was determined as the potential at which a sharp and sudden rise in the current density occurred and continues to rise. This procedure was repeated 20 times for each sample.

Table 1
Chemical composition of AISI 403 martensitic stainless steel used in this study.

C	Cr	Ni	Mn	Si	Cu	Mo	N	Co	V	P	S	Other	Fe
0.165	11.64	1.00	0.83	0.29	0.16	0.04	0.04	0.04	0.03	0.03	0.01	<0.01	Bal.

Table 2
Different solution compositions used for the DL-EPR investigations.

Solution number	Composition	Reference
1	0.1 M H_2SO_4 + 0.4 M Na_2SO_4 + 1000 ppm KSCN	[5]
2	0.5 M H_2SO_4	[7]
3	0.1 M H_2SO_4	–
4	0.01 M H_2SO_4 + 0.01 M KSCN	–
5	0.01 M H_2SO_4	–

The potentiostatic experiments were carried out in −100 mV vs. SCE. The time a stable pit required to create, was used for plotting a survival probability diagram, according to the Eq. (2).

$$\text{survival probability}\ (\%) = 1 - \left(\frac{n}{N+1}\right) \times 100 \qquad (2)$$

where N is the total number of repeated experiments, and n is the number of samples that showed pitting in a specific potential range.

The OCP measurement was performed for 1200 s to approach the steady state condition before each potentiodynamic and potentiostatic test.

3. Results and discussion

3.1. Degree of sensitisation (DOS) measurements

Fig. 2 shows the results of the DL-EPR experiments for as-quenched specimen and sample tempered at 550 °C performed in the various solutions listed in Table 2. Although, it is expected that as-quenched sample does not show any sign of sensitisation, a big loop in reverse scanning appeared in solutions 1, 2 and 3. However, in solution 5 only a negligible increase in I_r is observed in comparison with I_a.

As depicted in Fig. 2, the sample tempered at 550 °C shows the sensitisation behaviour. Mainly, because in DL-EPR tests, I_r represents a fraction of the material depassivated due to chromium depletion; therefore, the value of I_r must be lower than the value

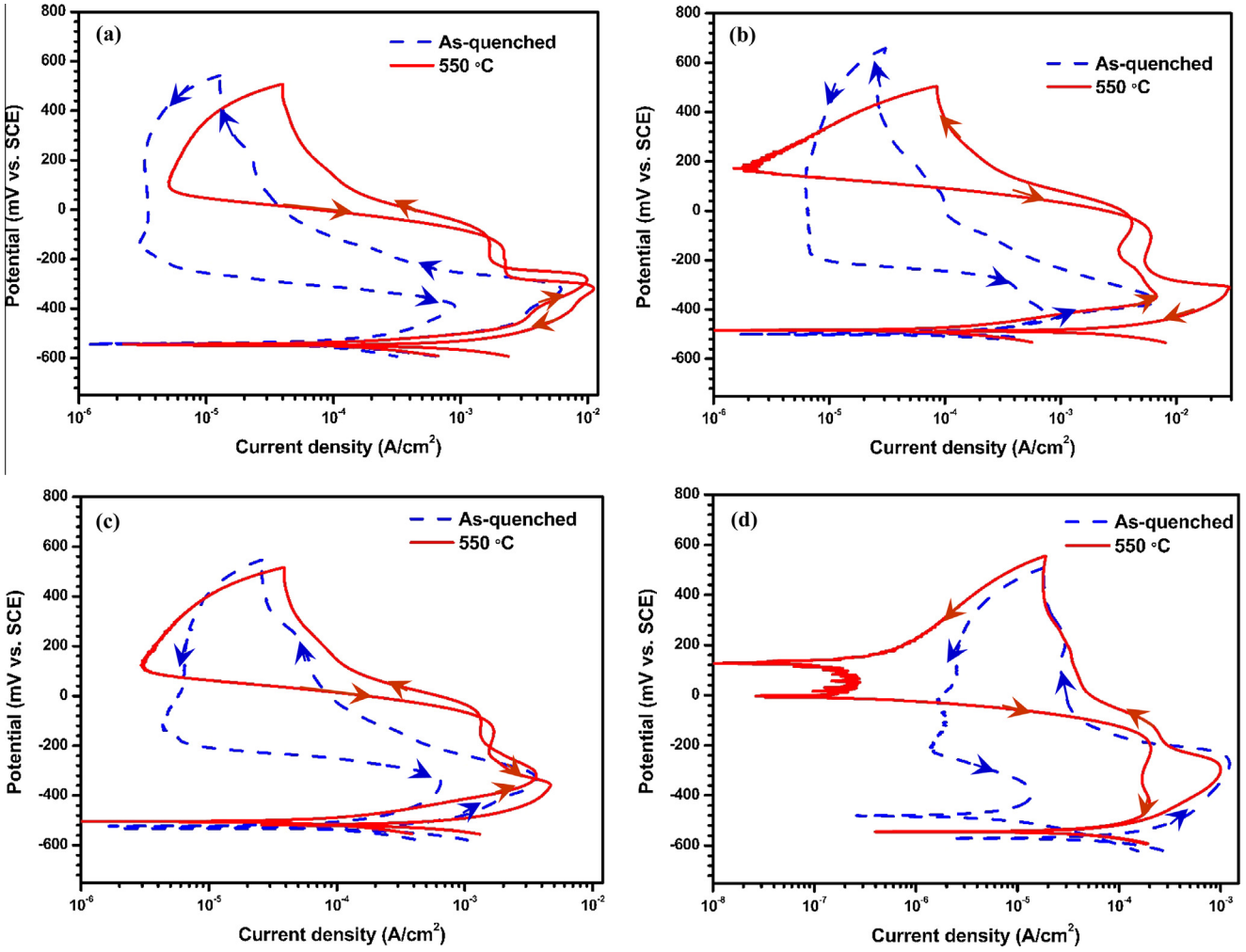

Fig. 2. DL-EPR diagrams of 403 martensitic stainless steel for as-quenched (dashed lines) and 550 °C tempered (solid lines) specimens obtained in various solutions: (a) 0.1 M H_2SO_4 + 0.4 M Na_2SO_4 + 1000 ppm KSCN, (b) 0.5 M H_2SO_4, (c) 0.1 M H_2SO_4, and (d) 0.01 M H_2SO_4.

Table 3
The values of the degree of sensitisation (DOS), calculated using Eq. (1) (DOS = Q_r/Q_a). The values Q_r and Q_a obtained from the DL-EPR experiments performed in 0.01 M H_2SO_4 solution with the scanning rate of 100 mV min^{-1} and the temperature of 20 °C.

Tempering temperature (°C)	DOS value (%)
As-quenched	0.8
300	0
450	0
550	40
650	2.8
750	0.6

of I_a [10]. Although the value of the reactivation current (I_r) in the case of solution 5 is lower than the activation current (I_a), the reverse loops of specimen tempered at 550 °C have exceeded the first loops in the solutions 1–3. On the other hand, solution 4 in which a regular amount of KSCN is presented did not show the passivity behaviour. Thus, for the low chromium martensitic stainless steels, KSCN utilised as a strong depassivator [11], is not appropriate for the DL-EPR experiments. Our investigations also showed that presence of H_2SO_4 at high concentrations is very corrosive for martensitic structures and consequently, is not proper for the DL-EPR tests. Therefore, the solution 5 is selected to the DL-EPR experiments for all different tempering conditions be performed.

Table 3 shows the DOS values obtained for various tempering conditions in the solution 5. As observed, the specimen tempered at 550 °C shows the highest DOS value of 40%. It is obvious that no sensitisation has occurred at the tempering temperatures below 550 °C. Therefore, it can be concluded that the formation of chromium carbides and consequently the chromium depleted zones is not probable in these conditions. On the other hand, due to initiation and growth of chromium carbides at samples tempered at temperatures above 450 °C, chromium depleted zones, especially at the grain boundaries, are formed. This is a probable reason for high degree of sensitisation of specimen tempered at 550 °C.

When the tempering temperature increases to 650 °C, the DOS declines and reaches to 2.8%, and completely vanishes by tempering at 750 °C. The occurrence of this phenomenon could be due to the chromium diffusion from the central areas of the grains to heal the depleted zones.

According to Lim et al. [3], the highest DOS of 403 martensitic stainless steel occurs when the alloy tempered at 660 °C for 1 h and tempering for 1 h at lower temperatures than 660 °C, would not be led to sensitisation. This discrepancy between our results and their work may return to the different natures of the applied methods of DOS measurements [5,6,12].

Fig. 3 shows the microstructural images obtained by optical microscope after electrochemical etching in oxalic acid. It indicates that, in the as-quenched sample and the specimens tempered below 550 °C, only the martensitic structure is revealed and no sign of intergranular sensitisation is observed (Fig. 3a–c). However, evidences of partial homogenous corrosion are also observed, which probably return to the initial inclusions and cannot be an indication of the sensitisation. These inclusions seem to be the reason of the dark corroded points observed in Fig. 3. Fig. 4 shows the SEM image and EDS diagram of this dark points representing the obvious peak of manganese and sulphur.

For the specimens tempered at 550 °C, the grain boundary corrosion is obvious which could be due to the chromium impoverishment and carbide formation in these regions (Fig. 3d). Poor passive layer and dissolution of carbides in the grain boundaries have led to a ditched structure which is etched by oxalic acid. Fig. 5 shows a higher magnification of the intergranular corrosion in the sensitised specimen tempered at 550 °C (Fig. 5b) in comparison with the non-sensitised one which is tempered at 300 °C (Fig. 5a).

3.2. Pitting measurements

Pitting potentials for all tempering temperatures were obtained by means of potentiodynamic polarisation in the 3.5 wt.% NaCl

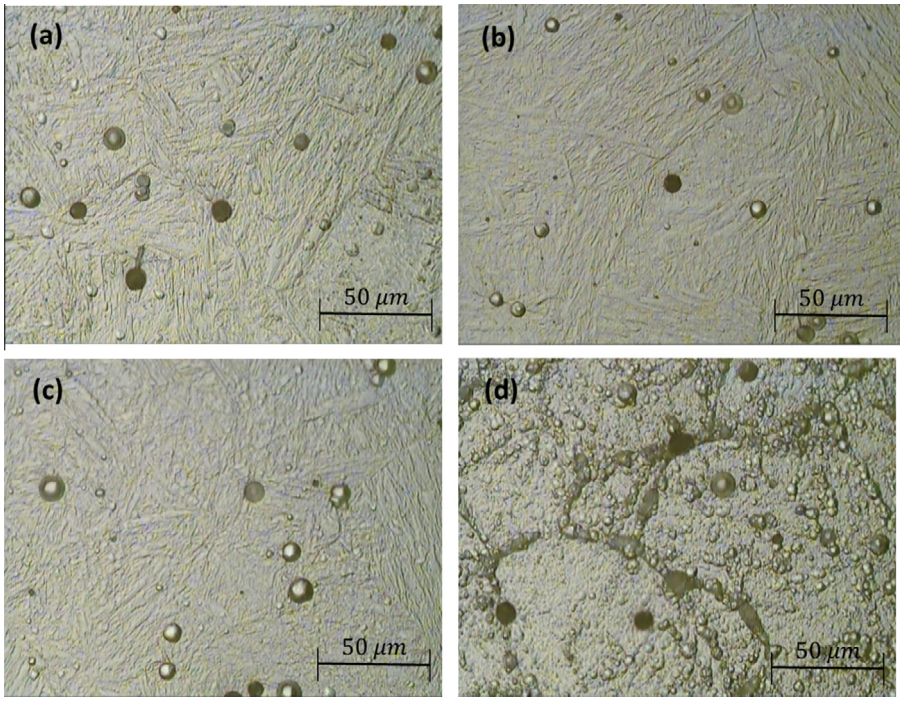

Fig. 3. Optical micrographs of solution annealed 403 martensitic stainless steel: (a) without tempering treatment and tempered at (b) 300 °C, (c) 450 °C and (d) 550 °C, after electroetching in 10 wt.% aqueous solution of oxalic acid for 90 s.

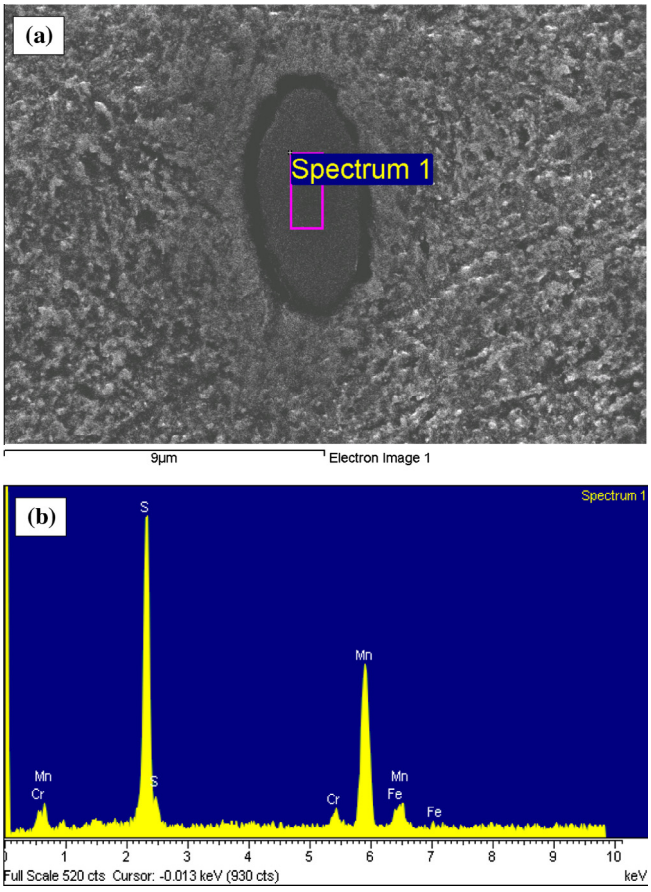

Fig. 4. SEM image (a) and EDS diagram (b) of dark points revealed after electroetching in 10 wt.% aqueous solution of oxalic acid for 90 s. The peaks of manganese and sulphur are observed obviously, that imply these particles are MnS inclusions.

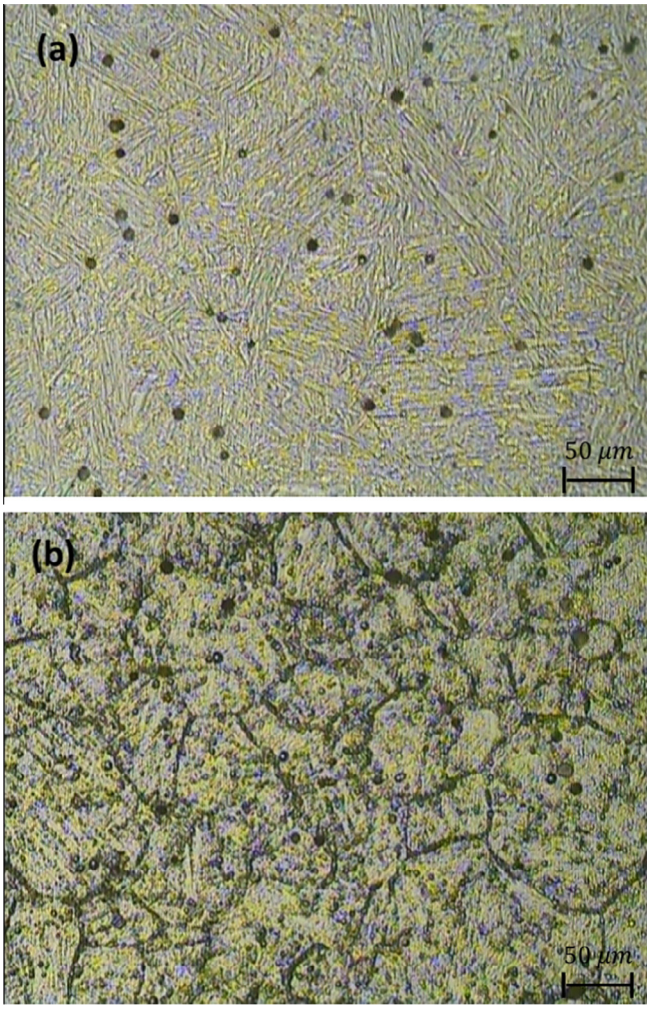

Fig. 5. Optical micrographs of 403 martensitic stainless steel specimens tempered at (a) 300 °C, (b) 500 °C after electroetching in 10 wt.% aqueous solution of oxalic acid for 90 s at a higher magnification.

solution. Fig. 6 illustrates the cumulative probability plots of the measured potentials. The graph shows the pitting probability, $P(E)$, as a function of potential, expressed as:

$$P(E) = \frac{n}{1+N} \tag{3}$$

where N is the total number of experiments and n is the number of pitted ones. Because the pitting potential of the 550 °C tempered specimen is lower than its corrosion potential, for this sample the probability of corrosion potential is plotted as a function of potential. In order to compare pitting potential of specimens in Fig. 6, one may consider the median values of pitting probability, i.e. $P(E) = 0.5$.

According to this diagram, the highest pitting potential belongs to the specimens tempered at 300 °C and 450 °C with the median pitting potential of 33 and 46 mV vs. SCE, respectively. It may be said that in the as-quenched specimen (with $E_{pit} = -26$ mV vs. SCE), there are many sheared martensitic laths providing a microstructure with high amount of residual stress. This stress, especially at the edges of inclusions, increases the susceptibility to the pitting corrosion [26–28]. Therefore, by rising the tempering temperature to 300 °C and 450 °C, the residual stresses of the martensite structure are released and the pitting corrosion behaviour of the specimen is improved. On the other hand, tempering at 550 °C decreases the pitting potential in a manner that the specimen begins to pitting at its corrosion potential. This behaviour

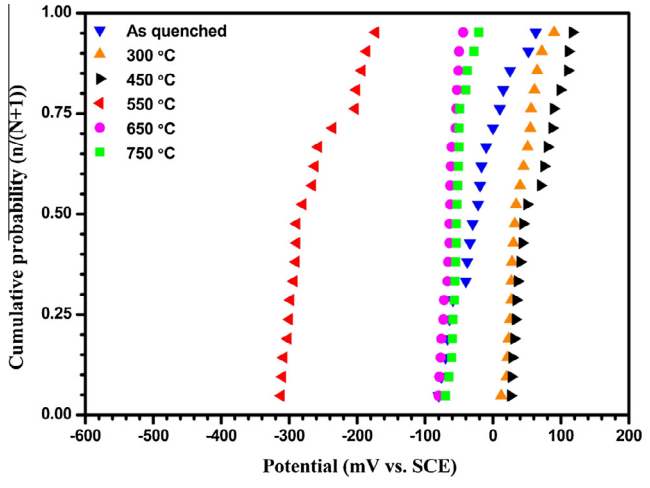

Fig. 6. Cumulative probability plots of the pitting potential for different tempering conditions of 403 martensitic stainless steel obtained from potentiodynamic polarisation tests performed in 3.5% NaCl solution at 20 °C. Because the pitting potential of the specimen tempered at 550 °C is lower than its corrosion potential, for this sample the corrosion potentials are depicted in the figure.

could be referred to the sensitisation of the steel occurred due to the carbide formation and consequently chromium depletion at this temperature. In fact, the chromium depletion and sensitisation

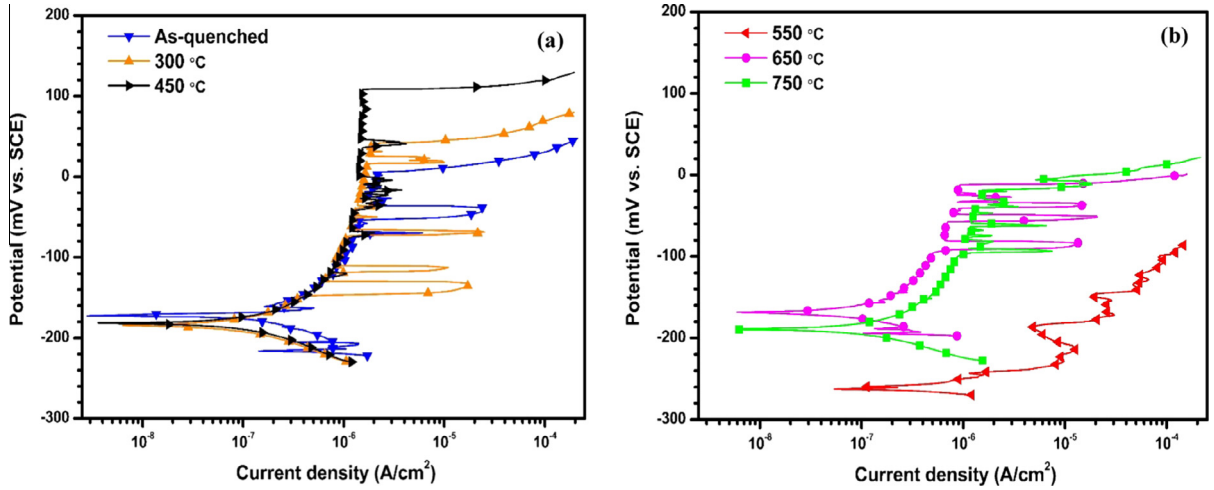

Fig. 7. Current density vs. potential plots obtained from potentiodynamic polarisation tests performed for different tempering conditions of 403 martensitic stainless steel in 3.5 wt.% NaCl solution at 20 °C.

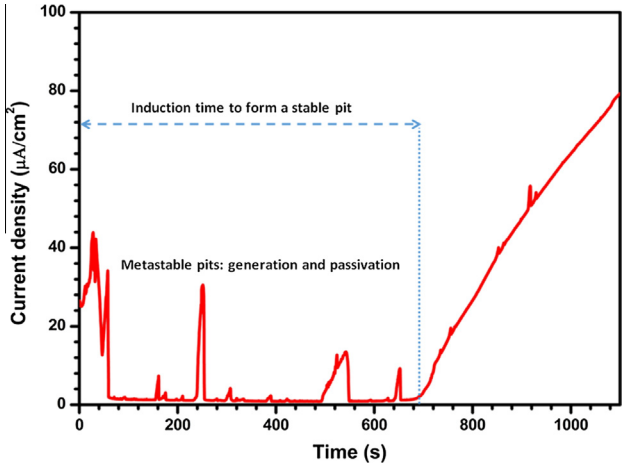

Fig. 8. Schematic diagram of potentiostatic polarisation for 403 martensitic stainless steel at the potential of −100 mV vs. SCE in 3.5 wt.% NaCl solution at 20 °C. The metastable pits and the induction time to form a stable pit are shown in the figure.

can accelerate the pitting corrosion by affecting both the pit nucleation and propagation.

It is well known that any discontinuity in the passive film can provide preferential sites for pit nucleation [24]. Because of the low content of chromium in this martensitic steel, any depletion of chromium at the grain boundaries can lead to weaken the passive film. This degradation is more severe when the amount of local chromium reaches to the values lower than 11% (i.e. least amount of chromium which is essential for steel to have stainless characteristic). Therefore, the regions adjacent to the grain boundaries can act as proper sites for pit nucleation [14].

Furthermore, it is generally accepted that in the stainless steels, pits usually initiate from inclusions [21–24]. These inclusions lead to the formation of metastable pits. Fluctuations observed in the potentiodynamic (Fig. 7) and potentiostatic (Fig. 8) polarisation curves, are referred to the formation, growth, and repassivation of the microscopic metastable pits [29–31]. It is claimed that the product of pit current density and pit depth should exceed a critical value to a metastable pit continue to grow and becomes a stable pit; otherwise, the pit would be repassivated [20,29,30,32]. In the case that a metastable pit nucleates in the chromium depleted zones, the pit current density will be higher due to the low concentration of chromium and therefore, the probability of stable pits formation increases.

As a result, the pitting potential in the sensitised specimen tempered at 550 °C is lower than the corresponding values of the specimens not tempered or tempered below 550 °C. This fact is illustrated in Fig. 7, in which, specimen tempered at 550 °C does not show passivity behaviour in the potentiodynamic polarisation and pitting corrosion occurs at corrosion potential (i.e. $E_{pit} < E_{Corr}$).

Fig. 9 shows the location of the pits formed on the surface of sensitised specimen (tempered at 550 °C) after the potentiodynamic polarisation. As observed, pits are more frequently formed at the grain boundaries. Thus, the grain boundaries are the most probable sites for both nucleation and growth of pits in the sensitised specimen. This could confirm the idea that the deterioration in pitting corrosion behaviour of the sensitised steel returns to the chromium depleted zones, which are mostly adjacent to the grain boundaries.

When the tempering temperature increases to 650 °C and 750 °C, the pitting potential again increases and reaches to −64 mV vs. SCE and −54 mV vs. SCE, respectively. However, these values are more than pitting potential of specimen tempered at 550 °C, but are moderately lower respect to the pitting potential of specimens tempered at temperatures below 550 °C. Therefore, it can be concluded that corrosion behaviour of specimens tempered at 650 °C and 750 °C is improved respect to pitting corrosion behaviour of specimen tempered at 550 °C. It could be because of the chromium diffusion to grain boundaries at relatively higher temperatures led to the chromium depleted zones healing. Although, the steel is healed at these temperatures, the total content of chromium is relatively low, as the carbide formation consumes chromium. Therefore, the pitting potential of the specimens tempered at 650 °C and 750 °C are moderately lower than the specimens which are tempered below 550 °C.

Fig. 10 shows the survival probability plots which measure an induction time (see Fig. 8) to form a stable pit at −100 mV vs. SCE for different conditions of tempering. As expected, the specimen which is tempered at 550 °C does not show any survivability at the applied potential of −100 mV vs. SCE. It means that the probability of formation of stable pits in this specimen is higher than other tempering conditions, which refers to the sensitisation. Furthermore, it is obvious that the specimens with tempering temperature of 300 °C and 450 °C have the highest survival probabilities. As depicted, 65% of the experiments of these two tempering conditions show the induction time greater than 120 min. Lower percent can

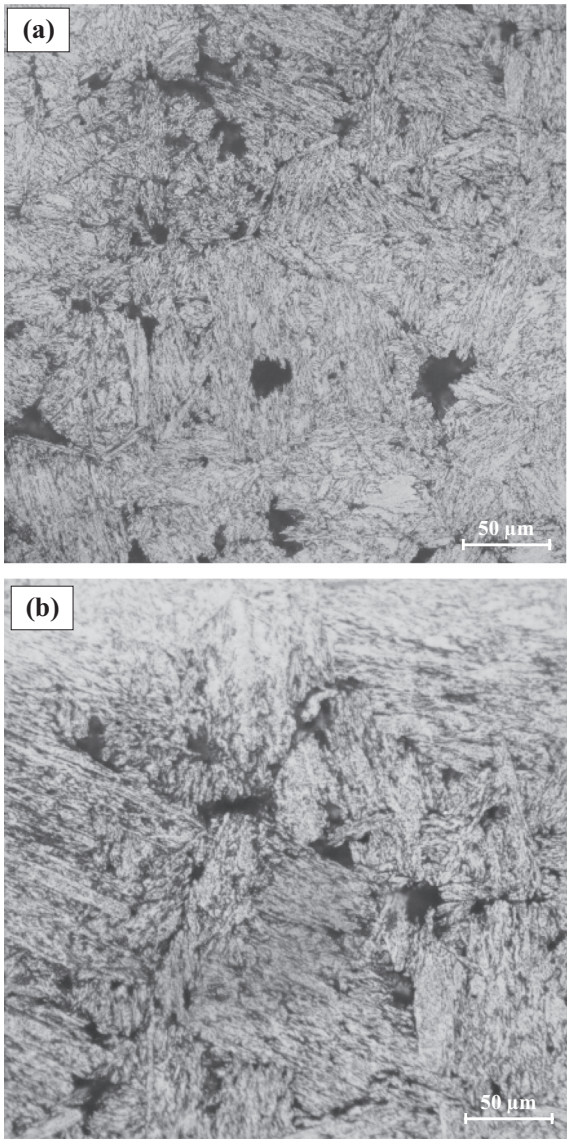

Fig. 9. Optical micrographs of sensitised 403 martensitic stainless steel specimen after performing potentiodynamic polarisation in 3.5 wt.% NaCl solution at 20 °C. Pits are more frequently nucleated and grown at the grain boundaries.

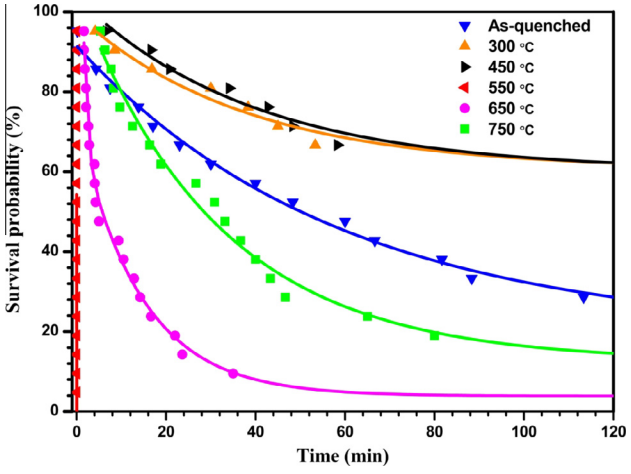

Fig. 10. Survival probability plots of 403 martensitic stainless steel specimens in different tempering conditions, obtained from the potentiostatic polarisations performed at −100 mV vs. SCE in 3.5 wt.% NaCl solution at 20 °C.

be observed for as-quenched, 650 °C and 750 °C treated samples, respectively. It is worth noting that the survival probability plots of all samples show a concave distribution with a long tail which is in agreement with literature [33].

4. Conclusion

In the present work, the DOS and pitting corrosion of 403 martensitic stainless steel is studied at different tempering conditions. Our investigations show that there is a correlation between sensitisation and pitting corrosion and the following results are obtained:

1. The standard test solution in DL-EPR method is not suitable for this type of stainless steel and cannot show the DOS properly. So the electrolyte is modified and the solution with the composition of 0.01 M H_2SO_4 is proposed.
2. DL-EPR experiments indicate that the specimens tempered at 300 °C and 450 °C are not sensitised. However the 550 °C tempered specimen shows the highest values of sensitisation with the DOS amount of 40%. For the specimens tempered at 650 °C and 750 °C the DOS values are decreased to 2.8% and 0.6%, respectively.
3. Potentiodynamic polarisations in 3.5 wt.% NaCl solution show that the passivity region does not appear in the specimen tempered at 550 °C. In other words, for this sample the corrosion potential is higher than the specimen pitting potential.
4. The results of potentiostatic polarisations indicate that the probability of formation of stable pits at constant potential is increased due to the sensitisation. Therefore the specimen with the DOS amount of 40% (tempered at 550 °C) has the lowest survival probability in comparison with other samples.
5. Microstructural studies demonstrate that pitting occurs more frequently at the grain boundaries in the sensitised specimens. Thus, it could be said that the grain boundaries in sensitised samples are the more probable sites for nucleation and growth of pits.

Acknowledgment

The authors acknowledge the financial support from Ferdowsi University of Mashhad/Iran provision of laboratory facilities during the period that this research was conducted.

References

[1] A.J. Sedriks, Corrosion of Stainless Steels, Wiley, New York, 1996.
[2] J.-Y. Park, Y.-S. Park, The effects of heat-treatment parameters on corrosion resistance and phase transformations of 14Cr–3Mo martensitic stainless steel, Mater. Sci. Eng. A 449–451 (2007) 1131–1134.
[3] L.C. Lim, M.O. Lai, J. Ma, D.O. Northwood, B. Miao, Tempering of AISI 403 stainless steel, Mater. Sci. Eng. A 171 (1993) 13–19.
[4] B. Miao, D.O. Northwood, L.C. Lim, M.O. Lai, Microstructure of tempered AISI 403 stainless steel, Mater. Sci. Eng. A 171 (1993) 21–33.
[5] S. Frangini, A. Mignone, Modified electrochemical potentiokinetic reactivation method for detecting sensitization in 12 wt% Cr ferritic stainless steels, Corrosion 48 (1992) 715–726.
[6] G.H. Aydoğdu, M.K. Aydinol, Determination of susceptibility to intergranular corrosion and electrochemical reactivation behavior of AISI 316L type stainless steel, Corros. Sci. 48 (2006) 3565–3583.
[7] N. Alonso-Falleiros, M. Magri, I.G.S. Falleiros, Intergranular corrosion in a martensitic stainless steel detected by electrochemical tests, Corrosion 55 (1999) 769–778.
[8] V. Kain, K. Chandra, K.N. Adhe, P.K. De, Detecting classical and martensite-induced sensitization using the electrochemical potentiokinetic reactivation test, Corrosion 61 (2005) 587–593.
[9] J.M. Aquino, C.A. Della Rovere, S.E. Kuri, Intergranular corrosion susceptibility in supermartensitic stainless steel weldments, Corros. Sci. 51 (2009) 2316–2323.

[10] S.S.M. Tavares, F.J. da Silva, C. Scandian, G.F. da Silva, H.F.G. de Abreu, Microstructure and intergranular corrosion resistance of UNS S17400 (17-4PH) stainless steel, Corros. Sci. 52 (2010) 3835–3839.
[11] A.P. Majidi, M.A. Streicher, The double loop reactivation method for detecting sensitization in AISI 304 stainless steels, Corrosion 40 (1984) 584–593.
[12] P. Novak, R. Stefec, F. Franz, Testing the susceptibility of stainless steel to intergranular corrosion by a reactivation method, Corrosion 31 (1975) 344–347.
[13] M. Momeni, A. Ale-yassin, M.H. Moayed, Establishing a new solution based on hydrochloric acid/sodium thiosulfate for detecting and measuring degree of sensitization of stainless steels using double-loop electrochemical potentiodynamic reactivation method, Corrosion 68 (2012) 015007-1–015007-11.
[14] A.S.M. Paroni, N. Alonso-Falleiros, R. Magnabosco, Sensitization and pitting corrosion resistance of ferritic stainless steel aged at 800 °C, Corrosion 62 (2006) 1039–1046.
[15] N. Ebrahimi, M. Momeni, M.H. Moayed, A. Davoodi, Correlation between critical pitting temperature and degree of sensitisation on alloy 2205 duplex stainless steel, Corros. Sci. 53 (2011) 637–644.
[16] J. Hong, D. Han, H. Tan, J. Li, Y. Jiang, Evaluation of aged duplex stainless steel UNS S32750 susceptibility to intergranular corrosion by optimized double loop electrochemical potentiokinetic reactivation method, Corros. Sci. 68 (2013) 249–255.
[17] D.L. Engelberg, 2.06 – intergranular corrosion, in: B. Cottis, M. Graham, R. Lindsay, S. Lyon, T. Richardson, D. Scantlebury, H. Stott (Eds.), Shreir's Corrosion, Elsevier, Oxford, 2010, pp. 810–827.
[18] V.r. Čihal, R. Štefec, On the development of the electrochemical potentiokinetic method, Electrochim. Acta 46 (2001) 3867–3877.
[19] G.S. Frankel, Pitting corrosion of metals a review of the critical factors, J. Electrochem. Soc. 145 (1998) 2186–2198.
[20] M.G. Alvarez, J.R. Galvele, 2.04 – pitting corrosion, in: B. Cottis, M. Graham, R. Lindsay, S. Lyon, T. Richardson, D. Scantlebury, H. Stott (Eds.), Shreir's Corrosion, Elsevier, Oxford, 2010, pp. 772–800.
[21] D.E. Williams, M.R. Kilburn, J. Cliff, G.I.N. Waterhouse, Composition changes around sulphide inclusions in stainless steels, and implications for the initiation of pitting corrosion, Corros. Sci. 52 (2010) 3702–3716.
[22] J. Stewart, D.E. Williams, The initiation of pitting corrosion on austenitic stainless steel: on the role and importance of sulphide inclusions, Corros. Sci. 33 (1992) 457–474.
[23] D.E. Williams, Y.Y. Zhu, Explanation for initiation of pitting corrosion of stainless steels at sulfide inclusions, J. Electrochem. Soc. 147 (2000) 1763–1766.
[24] G.T. Burstein, S.P. Vines, Repetitive nucleation of corrosion pits on stainless steel and the effects of surface roughness, J. Electrochem. Soc. 148 (2001) B504–B516.
[25] J.M. Aquino, C.A. Della Rovere, S.E. Kuri, Intergranular and pitting corrosion susceptibilities of a supermartensitic stainless steel weldment, Corrosion 66 (2010).
[26] D. Chastell, P. Doig, P.E.J. Flewitt, K. Ryan, The influence of stress on the pitting susceptibility of a 12%CrMoV martensitic stainless steel, Corros. Sci. 19 (1979) 335–341.
[27] P. Peyre, X. Scherpereel, L. Berthe, C. Carboni, R. Fabbro, G. Béranger, C. Lemaitre, Surface modifications induced in 316L steel by laser peening and shot-peening. Influence on pitting corrosion resistance, Mater. Sci. Eng. A 280 (2000) 294–302.
[28] R. Oltra, V. Vignal, Recent advances in local probe techniques in corrosion research – analysis of the role of stress on pitting sensitivity, Corros. Sci. 49 (2007) 158–165.
[29] P.C. Pistorius, G.T. Burstein, Growth of corrosion pits on stainless steel in chloride solution containing dilute sulphate, Corros. Sci. 33 (1992) 1885–1897.
[30] G.T. Burstein, P.C. Pistorius, S.P. Mattin, The nucleation and growth of corrosion pits on stainless steel, Corros. Sci. 35 (1993) 57–62.
[31] Y. González-García, G.T. Burstein, S. González, R.M. Souto, Imaging metastable pits on austenitic stainless steel in situ at the open-circuit corrosion potential, Electrochem. Commun. 6 (2004) 637–642.
[32] J.R. Galvele, Transport processes and the mechanism of pitting of metals, J. Electrochem. Soc. 123 (1976) 464–474.
[33] T. Shibata, W.R. Whitney Award lecture: statistical and stochastic approaches to localized corrosion, Corrosion 52 (1996) (1996) 813–830.